demonstrated [7,8,13,14]. Importantly, recent genetic linkage analyses have demonstrated the strongest association of serum levels of gp70-anti-gp70 immune complexes, rather than the levels of anti-dsDNA autoantibodies, with the development and severity of glomerulonephritis [15-18], suggesting a major pathogenic role of anti-gp70 autoantibodies in the lupus-prone mice. However, suggested pathogenicity of anti-gp70 autoantibodies had not been directly tested until recently. To examine if anti-gp70 autoantibodies induce glomerular and vascular pathology, we have established from unmanipulated MRL/lpr mice hybridoma clones that secrete monoclonal antibodies reactive with endogenous xenotropic viral env gene products [19,20]. A high proportion of these monoclonal anti-gp70 autoantibodies induced in syngeneic non-autoimmune (BALB/c x MRL/Mp-+/+)F1 and severe combined immunodeficiency (SCID) mice proliferative or wire loop-like glomerular lesions associated with massive gp70 deposition [20]. Furthermore, we found an IgG2a-producing anti-gp70 hybridoma clone that induced acute hemorrhagic death upon transplantation into syngeneic non-autoimmune mice. Subsequent analyses have demonstrated the binding of the anti-gp70 autoantibody onto mouse platelets, and induction of diffuse intraluminal platelet aggregation in mice transferred with this autoantibody [19].

In the present paper, we summarize our observations on the pathogenicity and molecular characteristics of the anti-gp70 autoantibodies, and report the development of vascular lesions in non-autoimmune mice by intravenous injection of a purified anti-gp70 autoantibody.

Materials and methods

Mice

Breeding pairs of MRL/MpJ-+/+ (MRL), MRL/lpr, and BALB/cCrSlc mice were purchased from Japan SLC, Inc., Hamamatsu, Japan, and (BALB/c x MRL)F_1 hybrid mice were bred in our animal facilities. NZW/NSlc and C57BL/6CrSlc (B6) mice were also purchased from Japan SLC, Inc. All the animal experiments described in this report were approved by and performed under the relevant guidelines of Kinki University.

Production and screening of hybridoma cells

For the screening of anti-gp70 autoantibodies, endogenous retroviral env genes and their chimeras were expressed by using recombinant vaccinia viruses as described [20]. A recombinant vaccinia virus expressing the influenza virus hemagglutinin (HA) gene [21] was used as a negative control throughout the experiment. Spleen and lymph node cells were prepared from

unmanipulated MRL/lpr mice and P3/NSI/1-Ag4-1 myeloma cells were used as fusion partner cells. Hybridoma cell fusion, hypoxanthine-aminopterin-thymidine selection, and cloning by colony formation in fibrin gels were performed as described previously [22,23]. For immunofluorescence detection of the reactivities of hybridoma-derived antibodies to expressed env gene products, monkey CV-1 cells were grown in wells of 96-well tissue culture plates, infected with a recombinant vaccinia virus at 100-200 plaque-forming units per well for 20-36 hours, and incubated at 4 °C, overnight with a hybridoma culture supernatant. After incubation, the cells in each well were washed with phosphate-buffered balanced salt solution (PBBS), fixed with methanol, blocked with 10 % skim milk, and were stained with a fluorescein isothiocyanate (FITC)-conjugated goat anti-mouse Ig antibody. Control hybridoma cell lines, N-S.7 producing anti-sheep red blood cell (SRBC) IgG3 and 2B12-2 producing anti-TNP IgM antibodies were used as negative controls.

Transfer of hybridoma cells or purified antibodies into non-autoimmune mice and pathological analyses in the recipients

(BALB/c x MRL)F_1 and SCID mice were transplanted intraperitoneally (i. p.) with 1-2 x 10^7 hybridoma cells after a pretreatment with a 0.5 ml/mouse i. p. dose of 2, 6, 10, 14-tetramethylpentadecane (pristane) given 1-3 weeks prior to hybridoma transplantation. For purification of a clonal anti-gp70 IgG, hybridoma cells were grown in a serum-free medium (Hybridoma SFM; Gibco BRL, Rockville, Maryland, U.S.A.) using 20-l spinner flasks, and culture supernates were concentrated by using a tangential flow ultrafiltration system. IgG was purified by Protein A-Sepharose affinity chromatography. Special attention was paid to perform the purification aseptically at room temperature, and to elute each antibody from the affinity column at pH = 4.4. Purified antibodies dissolved in PBBS at 0.5-1.0 mg/ml were injected into the tail vein after removing possibly contaminating Ig aggregates by centrifugation at 10,000 x g for 15 min. The methods for preparation and staining of formalin-fixed, paraffin-embedded tissue sections, preparation of specimens for electron microscopy, and immunohistochemical staining of frozen sections have been described [13,19,20,22,23].

Cloning and sequencing of Ig heavy and light chain cDNA

Total RNA was prepared from each clone of the hybridoma cells using the TRIzol reagent (Invitrogen Life Technologies, Carlsbad, California, U.S.A.) and mRNA was purified by using the poly(A)+ isolation kit (Nippon Gene, Tokyo, Japan). 5' RACE reaction was performed by using the SMART RACE cDNA Amplification kit (Clontech, Palo Alto, California, U.S.A.) with the following primers:

5'-GGGGAGGGCACTGACCACCCGGAGA-3' for Cγ2a,
5'-TTGGGGGGAAGATGAAGACGGATGG-3' for Cγ3, and
5'-TTGGTCAACGTGAGGGTGCTGCTCATGC-3' for Cκ.

The amplified full-length cDNA was purified by cutting the band out from agarose gel, and cloned into pGEM-T Easy vector (Promega Corporation, Madison, Wisconsin, U.S.A.), and resultant clones were subjected to DNA sequencing of each insert by using BigDye terminator v3.1 cycle sequencing kit (Applied Biosystems, Foster City, California, U.S.A.). Sequencing data were considered valid when > 8 independent plasmid clones with an identical sequence were observed.

Detection of serum gp70

For the detection of serum gp70, sera from NZW, (BALB/c × MRL)F1 and B6 mice were mixed at 1:20 with the SDS sample buffer containing no reducing agent, and serum proteins were separated through 7.5 % polyacrylamide gel and blotted onto polyvinylidenedifluoride membrane. After being blocked with 10 % skim milk, serum gp70 molecules were detected with a biotin-conjugate of anti-gp70 mAb 24-6 [24] by chemiluminescence reaction using horse radish peroxidase-conjugated streptavidin and ECL+ reagent (Amershan Pharmacia Biotech, Uppsala, Sweden) according to the manufacturers' instructions.

Results

Developement of glomerulonephritis in non-autoimmune mice transferred with monoclonal anti-gp70 autoantibodies. Sixteen independent hybridoma clones that produce antibodies reactive with the endogenous xenotropic viral gp70 were established by the fusion of B cells from unmanipulated MRL/lpr mice with the myeloma cells. These antibodies reacted with the cells infected with the recombinant vaccinia virus that expressed the endogenous retroviral env gene, but not with the cells infected with the vaccinia virus-influenza virus HA recombinant. Further analyses performed by using recombinant vaccinia viruses expressing reciprocal chimeras between the NZB xenotropic viral and polytropic Friend spleen focus-forming viral (SFFV) env genes indicated that 8 of these hybridoma antibodies are reactive with an epitope localized within the N-terminal one third of the xenotropic viral gp70, while two others require the presence of the C-terminal 2/3 of the xenotropic viral gp70 for their binding to the expressed antigens. Six other clones were cross-reactive to both the xenotropic viral and polytropic SFFV env gene products.

All these hybridoma clones were transplanted into syngenic, non-autoimmune (BALB/c x MRL)F1 mice, and 10 of them induced glomerular pathology of varying severity and morphology. Among them, two representative IgG3-producing clones, 12H5.1 and 37C4.1, induced the most severe glomerular pathology with the highest frequency but with distinct

morphological features. The lesions induced by the transplantation of clone 12H5.1 were characterized by the accumulation of inflammatory cells within the capillary lumina with numerous droplet-like granules within the cytoplasm of the infiltrated cells (Fig. 1). Deposits of an electron-dense material between the basement membrane and endothelial cells were also observed. Immunohistochemical analyses showed granular depositions of IgG, C3, and gp70, indicating the above glomerular deposits to be gp70-anti-gp70 immune complexes. On the other hand, the lesions induced by the transplantation of clone 37C4.1 were characterized by the massive and homogeneous subendothelial deposition of an electron-dense material, which resembled wire-loop lesions under light microscopy. The depositions of IgG, C3, fibrin, and gp70 were also observed. Four other clones, 37C6.1 (IgG2a), 51D1.1 (IgG3), 58C5.1 (IgM), and 60A5.1 (IgG3) also induced glomerular pathology with proliferative and/or sclerosing changes when transplanted into the syngeneic non-autoimmune mice with lower frequencies. Interestingly, clone 36D1.1, which did not induce glomerular pathology, instead induced hemorrhagic thrombocytopenia morphologically resembling the microvascular changes of human immune thrombocytopenic purpura. This antibody has been shown to react with a gp70-related membrane protein expressed on the surface of mouse platelets.

To exclude the possibility that hybridoma-derived cytokines and other cellular products were involved in the formation of glomerular pathology in the above transplanted animals, we next purified IgG from the cultures of representative anti-gp70 antibody-producing cells, and injected purified antibodies into non-autoimmune mice. Purified anti-gp70 IgG3 12H5.1, 37C4.1, and 51D1.1 induced glomerular pathology associated with thickening of capillary walls and increased cellularity. Depositions of gp70 were also demonstrated by immunohistochemistry in glomeruli of the mice injected with the purified anti-gp70 IgG. Severer glomerular pathology was induced when two anti-gp70 antibodies of separate epitope specificities, 12H5.1 and 51D1.1 were mixed and injected together.

Since mouse IgG3 lack allotypes, we next injected purified anti-gp70 IgG3 into three different strains of mice that differ in their amounts of constitutively expressed serum gp70. The same amount (3-4 mg/mouse) of purified anti-gp70 antibody 12H5.1 was injected into NZW, (BALB/c x MRL)F1, and B6 strains of mice, which express high, medium, and very low amounts of serum gp70, respectively. Glomerular pathologies with gp70 depositions were observed in antibody-injected NZW and the F1 mice, while no significant pathology was induced in the injected B6 mice (Fig. 1). These data indicated that the formation of gp70 immune complexes was involved in the development of glomerular pathology in anti-gp70 antibody-injected mice. By absorbing plasma immune complexes to Protein A-Sepharose and performing Western blot analyses of the Protein A-bound materials with labeled anti-gp70 monoclonal antibody, we actually detected the presence of gp70-containing immune complexes in mice injected with the purified anti-gp70 autoantibody (data not shown).

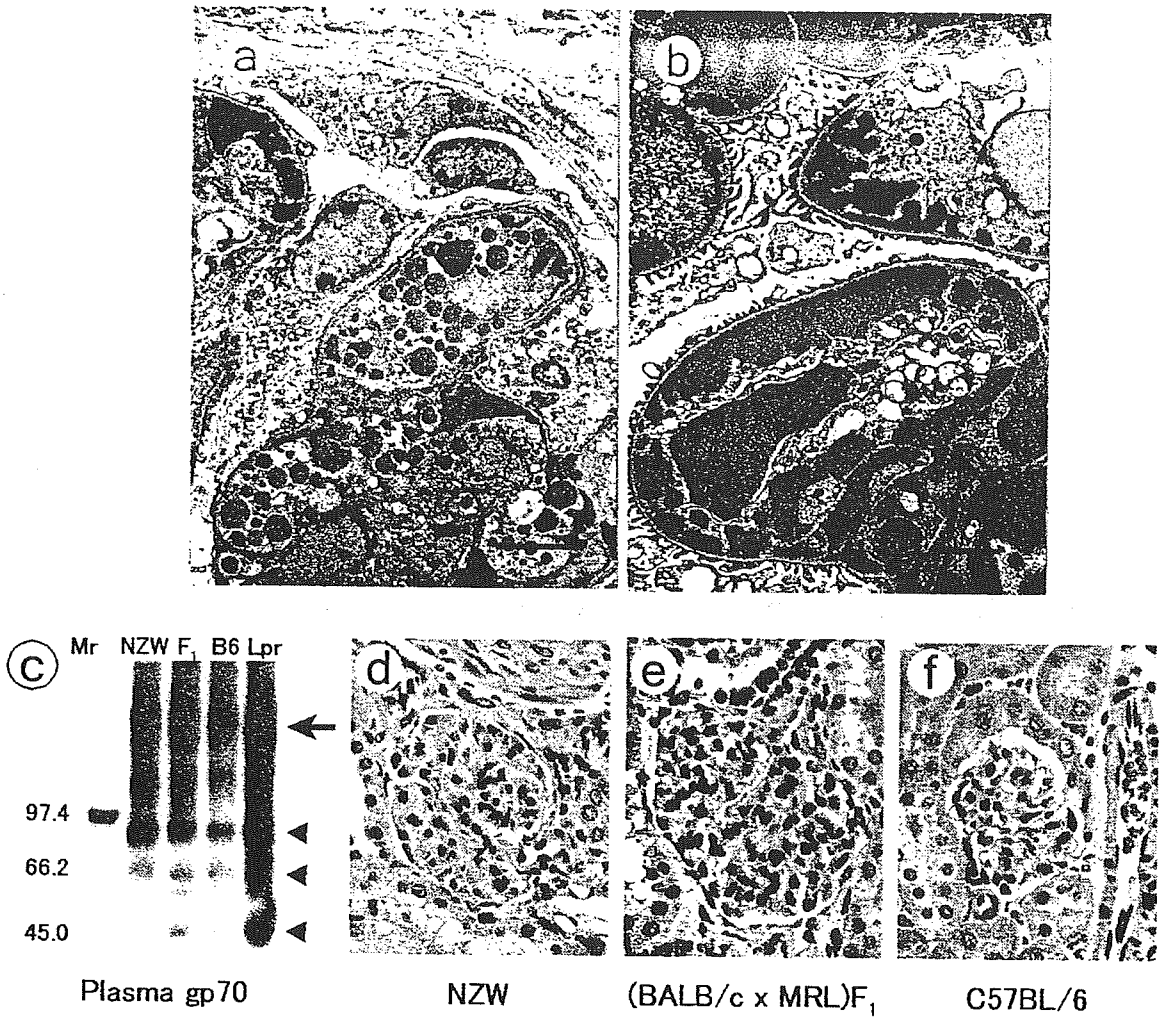

Fig. 1: Pathogenicity of monoclonal anti-gp70 autoantibodies established from MRL/lpr lupus mice shown by passive transfer into non-autoimmune mice. a, An electron micrograph showing cellular proliferation filling the glomerular capillaries and accumulation of electron-dense droplets in the cytoplasm of glomerular cells in (BALB/c x MRL)F1 mice transplanted with anti-gp70 antibody-producing hybridoma cell clone, 12H5.1. Bar = 5 mm. b, Massive deposition of electron-dense materials between the basement membrane and the endothelial cells in the glomeruli of a representative (BALB/c x MRL)F1 mouse transplanted with another anti-gp70 autoantibody-producing hybridoma cell line, 37C4.1. Bar = 2 mm. c, A representative western blot analysis showing differences in serum gp70 expression in NZW, (BALB/c x MRL)F1, and B6 mice. Sera were diluted 1:20 into the SDS-sample buffer without a reducing reagent, boiled for 5 min., and 10 ml of each boiled mixture was loaded into a well of 7.5 % polyacrylamide gel. Plasma from a 4 month-old female MRL/lpr mouse (Lpr) that should contain a large amount of gp70-anti-gp70 immune complexes, was used as a positive control. NZW mice expressed a high level of serum gp85 (gp70 + p15E), gp70, and a degradation product gp45 (arrowheads), while their expression in B6 mice was low. (BALB/c x MRL)F1 mice (F1) expressed an intermediate level of serum gp70. Mr, biotinylated markers with numbers on the left showing relative molecular mass x 10–3. The viral envelope gp70 is known to form trimers, and the corresponding band of apparent molecular mass > 220 kDa was observed (arrow). d-f, Representative photomicrographs taken from kidney sections of NZW (d), (BALB/c x MRL)F1 (e), and B6 (f) mice injected with purified anti-gp70 IgG3, 12H5.1.

Hematoxylin and eosin staining, x 300. Note apparent thickening of the capillary walls and inflammatory cell infiltration in d, and the marked increase in glomerular cellularity and evident neutrophilic infiltration in e.

Immunoglobulin variable region gene usage and amino acid sequences of the pathogenic anti-gp70 autoantibodies

Immunoglobulin heavy and light chain V gene usages and amino acid sequences of the above pathogenic anti-gp70 autoantibodies established from MRL/lpr lupus mice were analyzed by determining nucleic acid sequences of the cDNAs (Tab. 1). Four of the 5 examined clones were using the germ line VH558 family gene which is known to be preferentially used by many anti-DNA antibody clones, including those established from an MRL/lpr mouse [25,26]. VH7183 family gene that is used by the anti-gp70 clone 51D1.1 is also known to be used preferentially by anti-DNA antibodies in (NZB x NZW)F1 mice [26]. Accordingly, the heavy chain CDR1 and CDR2 amino acid sequences of the examined pathogenic anti-gp70 autoantibodies are similar to those reported for the anti-DNA antibody clones established from the MRL/lpr mouse. However, the observed amino acid sequences of heavy chain CDR3 of the pathogenic anti-gp70 antibodies were quite dissimilar to those reported for anti-DNA antibodies, suggesting that CDR3 is mainly involved in the determination of anti-gp70 specificity of these antibodies. In addition, a high frequency of Arg or Lys residues in CDR3 that is know to favor DNA binding of autoantibodies [26,27] was not a common feature of the examined anti-gp70 antibodies, and accumulation of these basic residues in CDR3 was observed in only two of the 5 examined clones. Interestingly, these 2 clones, 36D1.1 and 37C4.1, established from a single fusion, shared the identical heavy chain gene sequence and hence the CDR amino acid sequences, but differed in their light chain gene usages. These results suggest that the two clones have probably developed from a common pre-B cell. Further, since observed pathogenicities of the two clones were different, pathogenic potentials in these two clones of anti-gp70 autoantibodies might be determined by their light chain amino acid sequences. Further analyses are required to experimentally prove this possibility.

Induction of granulomatous arteritis by injection of purified anti-gp70 monoclonal antibody into non-autoimmune mice

During the process of examining glomerular pathology in anti-gp70 antibody-injected animals, we noted the presence of granulomatous arteritis in the lungs of some injected mice. The lesions were characterized by dense accumulation of neutrophyls and macrophage-like cells in the adventitia with focal destruction of the muscular media. Subendothelial accumulation of neutrophils in the intima was also observed, but less frequently. Small

arterioles were mainly involved, but larger branches of pulmonary arteries were also affected at a low frequency. To systemically analyze the development of this arterial pathology, we purified large amounts of the anti-gp70 and control anti-SRBC IgG3 antibodies, and injected them into (BALB/c x MRL)F1, (B6 x MRL)F1, and NZW mice. A total of 3-6 mg/mouse of a purified antibody was injected in 6 to 10 split doses of 0.7 ml twice a day for 3 to 5 days, and injected animals were examined 2 days after the final injection based on the results of preliminary experiments in which pathological analyses were done 1, 2, 4, and 7 days after the final injection. The granulomatous arterial lesions were observed only in mice injected with anti-gp70 clone 12H5.1, but not in those injected with 51D1.1 or control anti-SRBC IgG3, N-S.7. The frequency of the development of the arteritis was higher in NZB mice than in (BALB/c x MRL)F1, suggesting possible involvement of gp70-anti-gp70 immune complexes. More detailed analyses on the pathogenesis of this granulomatous arteritis are currently under way, and will be reported separately.

Tab. 1. Immunoglobulin variable region gene usage and deduced amino acid sequence of pathogenic anti-gp70 autoantibodies.

Clone	Isotype	V_H	J_H	$V\kappa_K$	$J\kappa_K$
12H5.1	IgG_3, κ	558	4	21	2
36D1.1	IgG_{2a}, κ	558	3	19-20	2
37C4.1	IgG_3, κ	558	3	8-21	4
37C6.1	IgG_{2a}, κ	558	3	10	2
51D1.1	IgG_3, κ	7183	4	21B	1

Clone	V_H		
	CDR1	CDR2	CDR3*
12H5.1	RYWMH	AIYPGNSDTSYNQKFKGK	EGISIYDGLYFAMDY
36D1.1	DYSMD	YIYPNNGYTGYNQKFKSK	**K**LG**RR**EAYFDV
37C4.1	DYYMD	YIYPNNDGTNYNQKFKGK	GGLAGYYLYYAMDY
37C6.1	DYSMD	YIYPNNGYTGYNQKFKSK	**K**LG**RR**EAYFDV
51D1.1	DYYMA	NINYDGSSTYYLDSLKSR	TPTGYYAMDY

Clone	V_L		
	CDR1	CDR2	CDR3
12H5.1	RASKSVSTSSYSYMH	YASYLES	QHSREFPYT
36D1.1	KASENVVTYVS	GASNRYT	GQGYSYPYT
37C4.1	KSTQSLFNSRTRKNYLA	WASTRES	TQSYYLH
37C6.1	RASQDISNYLN	YTSRLHS	QQYSKLPYT
51D1.1	RASKSVDRYGNSFMH	RTSNLES	QQNNEDPWT

*Basic amino acid residues within CDR3 are shown in boldface.

Discussion

Since the discovery of spontaneous mouse models of SLE, it has long been debated if anti-DNA antibodies are mainly responsible for the development of fatal nephritis, or anti-gp70 antibodies reactive to the endogenous retroviral env gene product play more important roles in the formation of the glomerular injury. Pathogenic potentials of anti-DNA antibodies have been shown in various experimental settings, but recent genetic analyses have indicated a closer correlation between the production of gp70-anti-gp70 immune complexes with the development of glomerulonephritis than that between the anti-DNA antibody production and fatal nephritis. We have shown here that monoclonal anti-gp70 autoantibodies established from MRL/lpr lupus mice are directly pathogenic when transferred into non-autoimmune mice. The deposition of gp70 in affected glomeruli along with IgG and C3, and the development of severer lesions in NZW mice that express higher concentrations of serum gp70 than B6 mice that developed no significant pathology indicate that gp70-anti-gp70 immune complexes are involved in the development of the glomerular pathology.

The pathogenic anti-gp70 autoantibodies used the same VH gene family as known anti-DNA antibody clones, but possessed unique CDR3 sequences that are dissimilar to those of anti-DNA antibodies. Further studies are required to conclude if antigen-driven somatic mutations are accumulated in the VH and VL genes of the anti-gp70 clones as has been reported for anti-DNA antibodies [25,27].

Vascular lesions of necrotizing and/or granulomatous types are frequently observed in mice predisposed to develop systemic autoimmune diseases [6-8,14]. However, pathogenesis of spontaneous vascular injury has been largely unknown. In a previous study, we have shown a close correlation between the presence of anti-gp70 autoantibodies and the development of necrotizing arteritis in SL/Ni strain of mice [14]. Vascular lesions were also induced in mice transplanted with the pathogenic anti-gp70 antibody-producing hybridoma cells as we reported previously [28] and in the present study. The development of granulomatous arteritis by the injection of purified anti-gp70 autoantibody is a unique phenomenon, and this model promises to be useful for the analyses of pathogenetic mechanisms of and the development of therapeutic means for human inflammatory vascular diseases.

Our model of vascular injury induced by the injection of anti-retroviral autoantibodies also suggests that immune responses to human retroviruses might be involved in the development of human inflammatory vascular diseases. This is particularly of interest because infections with exogenous human retroviruses, HTLV-I and HIV-1, are known to be associated with vasculitis [8,9]. Although sceptical views are common among retrovirologists on the possible involvement of human endogenous retroviruses in the pathogenesis of autoimmune diseases [11,12], it might be worth recalling that most retrovirologists had been sceptical to the point of nearly denying the

possibility of retroviruses playing a role in human cancers until HTLV-I was finally discovered [1].

References

1. Gallo RC. The early years of HIV/AIDS. Science 2002; 298: 1728-31.
2. Rahman A, Hiepe F. Anti-DNA antibodies – overview of assays and clinical correlations. Lupus 2002; 11: 770-773.
3. Smeenk RJT. Antinuclear antibodies: cause of disease or caused by disease? Rheumatology 2000; 39: 581-584.
4. Ravirajian CT, Rowse L, MacGowan JR, Isenberg DA. An analysis of clinical disease activity and nephritis-associated serum autoantibody profiles in patients with systemic lupus erythematosus: a cross-sectional study. Rheumatology 2001; 40: 1405-12.
5. Amoura Z, Piette J-C, Bach J-F, Koutouzov S. The key role of nucleosomes in lupus. Arthritis Rheum. 1999; 42: 833-843.
6. Andrews BS, Eisenberg RA, Theofilopoulos AN, et al. Spontaneous murine lupus-like syndromes. Clinical and immunopathological manifestations in several strains. J. Exp. Med. 1978; 148:1198-1215.
7. Theofilopoulos AN, Dixon FJ. Murine models of systemic lupus erythematosus. Adv. Immunol. 1985; 37:269-390.
8. Krieg AM, Steinberg AD. Retroviruses and autoimmunity. J. Autoimmun. 1990; 3:137-166.
9. Garry RF, Krieg AM, Cheevers WP et al. Retroviruses and their roles in chronic inflammatory diseases and autoimmunity. In: The Retroviridae. vol 4. New York: Plenum Press, 1995; 491-603.
10. Conrad B, Weissmahr RN, Boni J, et al. A human endogenous retroviral superantigens as candidate autoimmune gene in type I diabetes. Cell 1997; 90:303-313.
11. Stoye JP. The pathogenic potential of endogenous retroviruses: a skeptical view. Trends Microbiol. 1999; 7: 430.
12. Portis JL. Perspectives on the role of human endogenous retroviruses in autoimmune diseases. Virology 2002; 296: 1-5.
13. Izui S, Elder JH, McConahey PJ, Dixon FJ. Identification of retroviral gp70 and anti-gp70 antibodies involved in circulating immune complexes in NZB × NZW mice. J. Exp. Med. 1981; 153:1151-60.
14. Miyazawa M, Nose M, Kawashima M, Kyogoku M. Pathogenesis of arteritis of SL/Ni mice. Possible lytic effect of anti-gp70 antibodies on vascular smooth muscle cells. J. Exp. Med. 1987; 166: 890-908.
15. Vyse TJ, Drake CG, Rozzo SJ, et al. Genetic linkage of IgG autoantibody production in relation to lupus nephritis in New Zealand hybrid mice. J. Clin. Invest. 1996; 98:1762-1772.
16. Tucker RM, Vyse TJ, Rozzo S, et al. Genetic control of glycoprotein 70 autoantigen production and its influence on immune complex levels and nephritis in murine lupus. J. Immunol. 2000; 165: 1665-72.
17. Haywood ME, Vyse TJ, McDermott A, et al. Autoantigen glycoprotein 70 expression is regulated by a single locus, which acts as a checkpoint for pathogenic anti-glycoprotein 70 autoantibody production and, hence for the corresponding development of severe nephritis, in lupus-prone BXSB mice. J. Immunol. 2001; 167: 1728-33.

18. Rigby RJ, Rozzo SJ, Gill H, et al. A novel locus regulates both retroviral glycoprotein 70 and anti-glycoprotein 70 antibody production in New Zealand mice when crossed with BALB/c. J. Immunol. 2004; 172: 5078-85.
19. Hashimoto K, Tabata N, Fujisawa R, Matsumura H, Miyazawa M. Induction of microthrombotic thrombocytopenia in normal mice by transferring a platelet-reactive, monoclonal anti-gp70 autoantibody established from MRL/lpr mice: an autoimmune model of thrombotic thrombocytopenic purpura. Clin. Exp. Immunol. 1999; 119: 47-56.
20. Tabata N, Miyazawa M, Fujisawa R, et al. Establishment of monoclonal anti-retroviral gp70 autoantibodies from MRL/lpr lupus mice and induction of glomerular gp70 deposition and pathology by transfer into non-autoimmune mice. J. Virol. 2000; 74: 4116-26.
21. Smith GL, Murphy BR, Moss B. Construction and characterization of an infectious vaccinia virus recombinant that expresses the influenza hemagglutinin gene and induces resistance to influenza virus infection in hamsters. Proc. Natl. Acad. Sci. USA. 1983; 80:7155-7159.
22. Robertson MN, Miyazawa M, Mori S, et al. Production of monoclonal antibodies reacting with a denatured form of the Friend murine leukemia virus gp70 envelope protein: use in a focal infectivity assay, immunohistochemical studies, electron microscopy, and Western blotting. J. Virol. Methods 1991; 34:255-271.
23. Miyazawa M, Mori S, Spangrude GJ, et al. Production and characterization of new monoclonal antibodies that distinguish subsets of mink lymphoid cells. Hybridoma 1994; 13:107-114.
24. Portis JL, McAtee FJ, Cloyd MW. Monoclonal antibodies to xenotropic and MCF murine leukemia viruses derived during the graft-versus-host reaction. Virology 1982; 118: 181-190.
25. Swanson PC, Yung RL, Blatt NB, et al. Ligand recognition by murine anti-DNA autoantibodies. II. Genetic analysis and pathogenicity. J. Clin. Invest. 1996; 97: 1748-60.
26. Marion TN, Tillman DM, Krishnan MK, et al. Immunoglobulin variable-region structures in immunity and autoimmunity to DNA. Tohoku J. Exp. Med. 1994; 173: 43-64.
27. Jang YI, Stollar BD. Anti-DNA antibodies: aspects of structure and pathogenicity. Cell. Mol. Life Sci. 2003; 60: 309-320.
28. Miyazawa M, Tabata N, Fujisawa R, et al. Roles of endogenous retroviruses and platelets in the development of vascular injury in spontaneous mouse models of autoimmune diseases. Int. J. Cardiol. 2000; 75: S65-S73.

Acknowledgements

This work was supported in part by grants from the Ministry of Education, Culture, Sports, Science, and Technology of Japan. We thank Mr. M. Patrick Gorman for critically reading and correcting the manuscript.

International Immunology, Vol. 18, No. 1, pp. 183–198
doi:10.1093/intimm/dxh361

Peptide-induced immune protection of CD8$^+$ T cell-deficient mice against Friend retrovirus-induced disease

Hiroyuki Kawabata[1], Atsuko Niwa[1,3], Sachiyo Tsuji-Kawahara[1], Hirohide Uenishi[2], Norimasa Iwanami[1,4], Hideaki Matsukuma[1], Hiroyuki Abe[1], Nobutada Tabata[1,5], Haruo Matsumura[1] and **Masaaki Miyazawa[1]**

[1]Department of Immunology, Kinki University School of Medicine, 377-2 Ohno-Higashi, Osaka-Sayama, Osaka 589-8511, Japan
[2]Genome Research Department, National Institute of Agrobiological Science, Tsukuba, Ibaraki 305-8602, Japan

[3]Present address: Department of Pharmacology, Kinki University School of Medicine, Osaka-Sayama, Osaka 589-8511, Japan
[4]Present address: Division of Experimental Immunology, Institute for Genome Research, University of Tokushima, Tokushima 770-8503, Japan
[5]Present address: Department of Pediatrics, Kinki University School of Medicine, Osaka-Sayama, Osaka 589-8511, Japan

Keywords: B cell-deficient, β_2-microglobulin-deficient, CD4$^+$ T, epitope, vaccine

Abstract

CD8$^+$ CTLs and virus-neutralizing antibodies have been associated with spontaneous and vaccine-induced immune control of retroviral infections. We previously showed that a single immunization with an *env* gene-encoded CD4$^+$ T cell epitope protected mice against fatal Friend retrovirus infection. Here, we analyzed immune cell components required for the peptide-induced anti-retroviral protection. Mice lacking CD8$^+$ T cells were nevertheless protected against Friend virus infection, while mice lacking B cells were not. Virus-producing cells both in the spleen and bone marrow decreased rapidly in their number and became undetectable by 4 weeks after infection in the majority of the peptide-immunized animals even in the absence of CD8$^+$ T cells. In the vaccinated animals the production and class switching of virus-neutralizing and anti-leukemia cell antibodies were facilitated; however, virus-induced erythroid cell expansion was suppressed before neutralizing antibodies became detectable in the serum. Further, the numbers of virus-producing cells in the spleen and bone marrow in the early stage of the infection were smaller in the peptide-immunized than in unimmunized control mice in the absence of B cells. Thus, peptide immunization facilitates both early cellular and late humoral immune responses that lead to the effective control of the retrovirus-induced disease, but CD8$^+$ T cells are not crucial for the elimination of virus-infected cells in the peptide-primed animals.

Introduction

Understanding the types of immune responses associated with and responsible for effective control of viral infection is pivotal for the development of antiviral vaccines. We, along with other researchers, have been studying the requirements of different immune cell components and their regulation by host genetic factors utilizing the mouse model of Friend retrovirus infection. Friend retrovirus complex (FV) is composed of replication-competent Friend murine leukemia virus (F-MuLV) and defective spleen focus-forming virus (SFFV), the latter of which induces rapid growth and terminal differentiation of infected erythroid progenitor cells (1, 2). FV is known to induce fatal erythroleukemia associated with severe immunosuppression when inoculated into immunocompetent adult mice of susceptible strains (1, 3). Genotypes at both MHC class I and class II loci, along with those at a non-MHC locus located on chromosome 15, affect spontaneous immune resistance against FV-induced disease development which is phenotypically manifested by the regression of early splenomegaly and clearance of viremia (1, 4–8). As predicted, requirements of both CD4$^+$ and CD8$^+$ T cells for the above

Correspondence to: M. Miyazawa; E-mail: masaaki@med.kindai.ac.jp

Transmitting editor: K. Sugamura

Received 4 June 2005, *accepted* 28 October 2005

Advance Access publication 13 December 2005

spontaneous resistance have been demonstrated through antibody-mediated depletion of T cell subsets and through the blocking of T cell responses by administration of anti-MHC class II antibodies (9, 10). Further, different roles of $CD4^+$ and $CD8^+$ T cells and of virus-neutralizing antibodies have been demonstrated for immune protection against FV infection induced with a live attenuated vaccine (11, 12).

We previously showed that a single immunization with an 18-mer peptide that contains a single $CD4^+$ T cell epitope identified within the *env* gene product SU of F-MuLV induces strong protective immunity against fatal FV infection in susceptible strains of mice (13, 14). In peptide-immunized (B10.A × A.BY)F_1 mice, the vast majority of virus-producing cells were eliminated from the spleen between 8 and 12 days after FV challenge, and the SFFV-induced early splenomegaly regressed rapidly. Production and class switching of virus-neutralizing antibodies roughly coincided with the above reduction in the number of virus-producing cells in the spleen (13), suggesting the possible importance of virus-neutralizing antibodies in the vaccine-induced confinement of FV infection. However, since the activation of both $CD4^+$ and $CD8^+$ cytotoxic effector cells and of NK cells was detectable prior to the decrease of virus-producing cells in peptide-immunized (BALB/c × C57BL/6)F_1 ($CB6F_1$) mice (14), it was also possible that the cellular responses, rather than the antibodies, were mainly responsible for the control of FV-induced disease development conceivably through the destruction of virus-producing cells. Moreover, since $CD8^+$ CTLs and NK cells were activated in comparable degrees both in peptide-immunized and unimmunized animals after FV infection (14), their actual extents of contribution to the peptide-induced immune protection remained unclear.

To directly evaluate the role of each separate immune cell component in peptide-induced protection against FV infection and to compare the effector mechanisms induced by the peptide immunization with those induced by previously described live attenuated vaccines (11, 15), we performed the protection experiments on the highly susceptible strain of mice that lacked either $CD8^+$ T or B lymphocytes.

Methods

Mice

BALB/c-AJcl and $CB6F_1$ mice were purchased from Japan SLC, Inc., Hamamatsu, Japan. (B10.A × A.BY)F_1 mice were those described previously (13). Breeding pairs of BALB/c-J-$B2m^{tm1Unc}$ and C57BL/6J (B6)-$B2m^{tm1Unc}$ mice carrying homozygous disruption of the β_2-microglobulin gene ($\beta_2m^{-/-}$) were purchased from the Jackson Laboratory, Bar Harbor, ME, USA, and F_1 crosses were produced at the Animal Facilities, Kinki University School of Medicine. Phenotypic lack of $CD8^+$ T cells in the produced F_1 crosses was confirmed by bleeding each mouse from the tail vein and staining peripheral blood with a mixture of fluorescence-labeled anti-CD4 and anti-CD8 mAbs as described in the following section.

B6-*Igh-6*^{tm1Cgm} mice carrying homozygous disruption of the membrane exon of the Ig μ-chain gene (μ-chain membrane exon-targeted: *μMT/μMT*) and thus lacking B cells (16) were also purchased from the Jackson Laboratory. To introduce the μ-chain disruption into BALB/c background, a cross-intercross production of a congenic strain was performed as follows: the B cell-deficient B6 male mice were mated with BALB/c female mice and F_1 crosses carrying heterozygous disruption of the μ-chain membrane exon were obtained. These heterozygous F_1 crosses were cross-mated, and F_2 mice carrying the homozygous μ gene disruption were selected by performing both genetic and phenotypic analyses as described below. The homozygous disruption of the μ-chain membrane exon in the resulting F_2 crosses was confirmed by PCR analyses as follows: genomic DNA was prepared from the tail tip of each mouse using DNeasy Tissue Kit (Qiagen GmbH, Hilden, Germany) according to the manufacturer's instructions. Oligo-DNA primers (5′ primer: 5′-TCTATCGCCTTCTTGACGAG-3′, 3′ primer: 5′-TACAGCTCAGCTGTCTGTGG-3′) were prepared based on the sequence information on the knockout cassette (16) and were used for PCR amplification of genomic DNA fragments. PCR products were separated by electrophoresis in a 4% agarose gel and were visualized under a UV light after ethidium bromide staining. In addition to the above genetic analyses, peripheral blood was stained with a mixture of fluorescence-labeled anti-CD3 and anti-CD19 mAb, and multicolor flow cytometric analyses were performed as described in the following section. Male F_2 mice carrying homozygous disruption of the μ-chain membrane exon and thus lacking B cells were mated with BALB/c female mice again, and this cross-intercross mating procedure was repeated seven times. After the seventh cycle of crossing and intercrossing, the resultant BALB/c-background mice possessing homozygous disruption of the μ-chain gene were maintained by sister–bother mating, and $CB6F_1$ mice lacking B cells were produced by crossing the B6-*Igh-6*^{tm1Cgm} and the above-established BALB/c-*μMT/μMT* mice.

For immune protection experiments, both male and female mice aged 8–11 weeks at the time of immunization were used throughout the present study. All the animal experiments were approved by the Animal Experiment Committee and performed under the guidelines of Kinki University.

Viruses and their inoculation

A stock of B-tropic FV complex was originally given by Bruce Chesebro, Laboratory of Persistent Viral Diseases, National Institute of Allergy and Infectious Diseases, Hamilton, MT, USA. The stock used in the present study has been described (14, 17). SFFV and F-MuLV titers of the FV stock were determined as described previously (13, 18). For inoculation into $CB6F_1$ mice, a dilution of the virus stock prepared with phosphate-buffered balanced salt solution (PBBS) containing 2% fetal bovine serum (FBS) was injected intravenously into the tail vein. Infected mice were observed at least twice a day and the number of surviving mice was determined. The development of splenomegaly was monitored by palpation as described (5, 17, 19). In some experiments, moribund mice were killed by cervical dislocation and spleen weights were measured to compare the results of palpation with actual spleen weights. Spleens weighing >0.5 g were consistently marked as palpable splenomegaly. Mice found dead were

dissected, and their spleen weight was measured to confirm leukemic death.

Peptide synthesis and immunization

The peptides used for detailed mapping of the $CD4^+$ T cell epitope were synthesized by Fmoc chemistry and purified, and their molecular weight confirmed by quad-polar mass spectrometry as described previously (20–22). Peptides used for immune protection experiments were ordered from Qiagen K. K. (Tokyo, Japan). For immunization each peptide was dissolved in PBBS and emulsified with an equal volume of CFA (Difco Laboratories, Detroit, MI, USA). Mice were injected intradermally with 100 µl of the emulsion given as multiple split doses into the abdominal wall. Control mice were given an emulsion of PBBS and CFA that did not contain any peptide.

T cell proliferation assays

Two T cell clones, F5-5 and FP7-11 (20, 23), specific for the $E^{b/d}$-restricted C-terminal epitope of F-MuLV *env* gene product were maintained as described previously (20). For examination of proliferative responses, 2×10^5 spleen cells irradiated with 40 Gy γ-ray were mixed with 2×10^5 T cells and various concentrations of a peptide in a well of 96-well microculture plates. After 48 h of incubation at 37°C, each culture was pulsed with 18.5 kBq [^{3}H]thymidine (Du Pont NEN, Boston, MA, USA) for the final 18 h. Cells were harvested onto a glass fiber filter, and incorporated radioactivity was measured with a microplate scintillation counter (TopCount, Packard Instrument Co., Meriden, CT, USA). For the calculation of relative stimulatory effect of each peptide, the concentration of peptide i (µM) required to induce 50% of the maximum proliferative response (ED_{50}) was divided with ED_{50} (µM) of the peptide in question (22, 23). In the present study proliferative responses were measured for a range of peptide concentrations between 0.01 and 20 µM in 2-fold dilutions, and peak responses (>30 000 counts per minute) were observed by stimulation with 1 µM of peptide i. ED_{50} of peptide i was 0.2 µM.

Assays for virus-neutralizing antibodies

The *in vitro* assays for quantitative measurement of F-MuLV-neutralizing antibodies have been described elsewhere in detail (5, 13, 17, 19). Mice were bled from the tail vein under ether anesthesia and sera separated were stored at −30°C until use. Stock of an infectious molecular clone of F-MuLV, FB29 (24), was prepared from a high-producer clone of chronically infected *Mus dunni* cells. Serial 2-fold dilutions of sera were made with PBBS containing 1% FBS and mixed with an appropriate dilution of the F-MuLV stock and inoculated to *Mus dunni* cells in 24-well plates. Control wells were inoculated with the virus dilution admixed with the diluent alone. Two days later, foci of F-MuLV-infected cells were visualized with mAb 720 (18) and counted under a dissecting microscope. Neutralizing titers were determined by the reciprocals of maximum dilutions that gave a reduction in the number of F-MuLV-infected cell foci to <25% of those in the control wells. IgG titers were determined by treating each serum sample with 0.05 M 2-mercaptoethanol whereas IgM titers were calculated by dividing the neutralizing titers of the untreated sera by the corresponding IgG titers (6).

Infectious center assays

These assays were performed as described previously (13, 17). Briefly, spleen and bone marrow cell suspensions prepared from mice challenged with FV were serially diluted with PBBS containing 2% FBS, plated in triplicate at concentrations between 30 and 3×10^6 cells per well onto monolayers of *Mus dunni* cells that had been seeded at 1.0×10^4 cells ml^{-1} per well on the previous day and then co-cultured for 2 days. After washing with PBBS and fixation with methanol, F-MuLV-infected cell foci were stained with mAb 720 (18), visualized by using the avidin-biotinylated peroxidase complex (Vector Laboratories, Burlingame, CA, USA) and counted under a magnifier. The numbers of detected foci are in linear correlation with the numbers of spleen cells inoculated in the range between 30 and 3×10^6 cells per well. For the plating of the whole spleen cells from each mouse, 5×10^6 spleen cells per well were added similarly to the previously started culture of *Mus dunni* cells in 20 wells of a 24-well plate, and the remaining spleen cells were diluted and plated at 5×10^5 and 5×10^4 cells per well into separate wells.

Flow cytometry

Flow cytometric analyses of cell-surface markers were performed as described elsewhere (14, 17, 25). Spleen and bone marrow tissues were dissociated in PBBS containing 2% FBS, and a single-cell suspension was prepared by passing each dissociated tissue through a nylon mesh. Cells were stained with a combination of the following mAbs, washed three times with PBBS containing 2% FBS and 0.05% NaN_3 and stained with 20 µg ml^{-1} 7-aminoactinomycin D (7-AAD). 7-AAD was used to exclude dead cells (26). The mAbs and their final concentrations used in the present study were: cychrome-conjugated anti-mouse CD3 (hamster IgG, PharMingen, San Diego, CA, USA) at 0.5 µg per 10^6 cells, FITC-conjugated anti-mouse CD4 (rat IgG2b, Seikagaku Corporation, Tokyo, Japan) at 0.5 µg per 10^6 cells, R-PE-conjugated anti-mouse CD8 (rat IgG2a, Caltag Laboratories, Burlingame, CA, USA) at 1 µg per 10^6 cells, PE-conjugated anti-mouse CD19 (rat IgG2a, PharMingen) at 1 µg per 10^6 cells, FITC-conjugated anti-mouse CD69 (hamster IgG, PharMingen) at 1 µg per 10^6 cells and allophycocyanin-conjugated anti-mouse TER-119 (PharMingen) at 0.2 µg per 10^6 cells. TER-119 reacts with a molecule associated with glycophorin A, and marks the late erythroblasts and mature erythrocytes, but not burst-forming and colony-forming units of erythroid cells (27). Biotinylated mAb 720 (IgG1) and 514 (IgM) used for the detection of F-MuLV gp70 and SFFV gp55, respectively, on infected cell surfaces has been described (13, 17). mAb 34 (IgG2b) reactive with the p15 (MA) protein (28) was similarly purified and biotinylated to detect cell-surface expression of the *gag* gene products (19). All staining reactions were performed in the presence of 0.25 µg per 10^6 cells anti-mouse CD16/CD32 (PharMingen) as described previously (25) to prevent the binding of mAb to FcR-expressing cells. Isotype-matched control antibodies were either purchased from the same suppliers or prepared as purified and biotinylated Ig of an irrelevant specificity as described (25), and staining patterns obtained with the negative-control antibodies were used to draw demarcation lines between cells positively stained and

those not stained. Multicolor flow cytometric analyses were performed with a Becton Dickinson FACSCalibur and CellQuest software (Becton Dickinson Immunocytometry Systems, San Jose, CA, USA). Mature erythrocytes and dead cells were excluded from the analyses by setting a polygonal gate in the dot plots showing intensities of forward scatter and fluorescence for 7-AAD.

Titration of serum antibody reactive to the surface of FV-induced leukemia cells

Sera were serially diluted between 1/4 and 1/256 with PBBS and 100 µl of each dilution was incubated with 10^6 FV-induced leukemia cells Y57-2C ($H2^{b/b}$). Characteristics of the leukemia cell line used in the present study have been described (14). After washing twice with PBBS containing 2% FBS, bound IgM and IgG were differentially detected by incubating the cells either with FITC-conjugated anti-mouse IgM (µ-chain specific, Southern Biotechnology Associates, Inc., Birmingham, AL, USA) at 5 µg per 10^6 cells or with FITC-conjugated anti-mouse IgG (γ-chain specific, Zymed Laboratories, Inc., South San Francisco, CA, USA) at 1.5 µg per 10^6 cells, respectively, for 20 min. Stained cells were washed three times before being examined by flow cytometry as described above.

Purification of T cells and their transfer

Purification of T cell subsets from the spleen of naive, immunized and/or FV-infected mice was performed by using mAb-conjugated magnetic microbeads and a magnetic cell sorter I (Miltenyi Biotec GmbH, Bergisch Gladbach, Germany) according to the manufacturer's instructions. Spleen cells were first treated with Tris-buffered ammonium chloride solution to lyse erythrocytes, and incubated with anti-B220 mAb-conjugated magnetic beads to remove B cells by passing through a negatively selecting CS column. To purify $CD4^+$ T cells, $B220^-$ cells were then incubated with anti-CD8 mAb-conjugated magnetic beads, passed through a CS column to remove $CD8^+$ cells and then incubated with anti-CD4 mAb-conjugated microbeads to positively select $CD4^+$ cells by passing through a VS column. Multicolor flow cytometric analyses revealed that the resultant cell preparation was >99% $CD4^+$. $CD8^+$ cells were similarly purified from $B200^-$ cells by removing $CD4^+$ cells and positively selecting $CD8^+$ cells. This preparation was 97–98% $CD8^+$ in repeated experiments. Percentages of $CD4^+$ and $CD8^+$ T cells in the spleen after FV inoculation were determined by flow cytometry in $CB6F_1$ mice immunized with peptide i. To reconstitute the full number of T cells that belonged to each subset in the immunized mice, unimmunized recipient mice were injected intravenously with 2×10^7 to 2.5×10^7 $CD4^+$ or $CD8^+$ T cells per mouse.

Depletion of $CD4^+$ T cells

Anti-mouse CD4 mAbs were purified from culture supernatant of the hybridoma cell GK 1.5 (29) as described previously (13, 25). Control rat myeloma IgG was purchased from Zymed Laboratories, Inc. The amount of the mAbs required for complete depletion of $CD4^+$ T cells from $CB6F_1$ mice was determined by intravenously administering the purified mAb and monitoring the number of $CD4^+$ and $CD8^+$ cells in the spleen by flow cytometry. The schedule of mAb administration finally adopted was as follows: $CB6F_1$ mice were immunized with 3 µg per mouse of peptide i emulsified in CFA. Three weeks later, mice were intravenously given 125 µg per mouse purified anti-CD4 mAb. Five additional intravenous doses of 125 µg per mouse anti-CD4 mAb were given 2, 4, 6, 9 and 18 days after the first administration. The negative-control rat IgG was given to a separate group of mice on the same schedule. Mice were inoculated with 150 spleen focus-forming units (SFFU) FV 7 days after the beginning of the mAb administration. Peripheral blood was collected from three representative animals at each time point through the tail vein at post-infection day (PID) 3, 6, 10 and 13, and flow cytometric analyses were performed to confirm the absence of $CD4^+$ T cells.

Statistical analyses

Differences in survival curves expressed by the Kaplan–Meier method were compared by a Mantel–Haenszel logrank test using GraphPad Prism 3 (GraphPad Software, Inc., San Diego, CA, USA). The numbers of mice that developed or lacked splenomegaly were compared between the immunized and unimmunized groups by Fisher's exact test. Average numbers of infectious centers between experimental groups and anti-leukemia cell antibody titers were compared by Mann–Whitney's *U*-test because these values were not expected to follow a Gaussian distribution. Differences in IgM and IgG titers of virus-neutralizing antibodies were compared by paired *t*-test. Spleen weights and percentages of $TER\text{-}119^+$, $gp70^+$ cells in the spleen and bone marrow between the immunized and unimmunized groups of mice were compared by Student's or Welch's *t*-test depending on whether the variances of the compared samples were estimated to be equal or not.

Results

Suppression of the early growth of FV-infected erythroid cells and prevention of leukemic death in highly susceptible $CB6F_1$ mice by immunization with a single-epitope $CD4^+$ T cell vaccine

Mice of BALB/c background are extremely susceptible to FV-induced disease, and $CB6F_1$ mice all died within 60 days after infection with only 15 SFFU of FV without showing any signs of spontaneous recovery (Fig. 1a). This was striking because even (B10.A × A/WySn)F_1 mice that have been used as a strain typically susceptible to FV infection have shown mortality rates of 70–80% at 90–100 days after inoculation with 15 SFFU FV (1, 5). Therefore, the following immune protection experiments were performed in $CB6F_1$ mice with 150 SFFU of FV to ensure that peptide-induced immune responses protect this highly susceptible strain of mice from doses of FV large enough to kill all unimmunized animals.

The efficacy of peptide i in priming $CD4^+$ T cells *in vivo* has been demonstrated by the establishment of $CD4^+$ T cell clones reactive to this peptide from the peptide-immunized $CB6F_1$ mice (23), and by more pronounced expansion of $CD4^+$ T cells in the spleen after FV challenge in the peptide-immunized than in the unimmunized control $CB6F_1$ mice (14). To directly demonstrate the priming of $CD4^+$ T cells in peptide-immunized

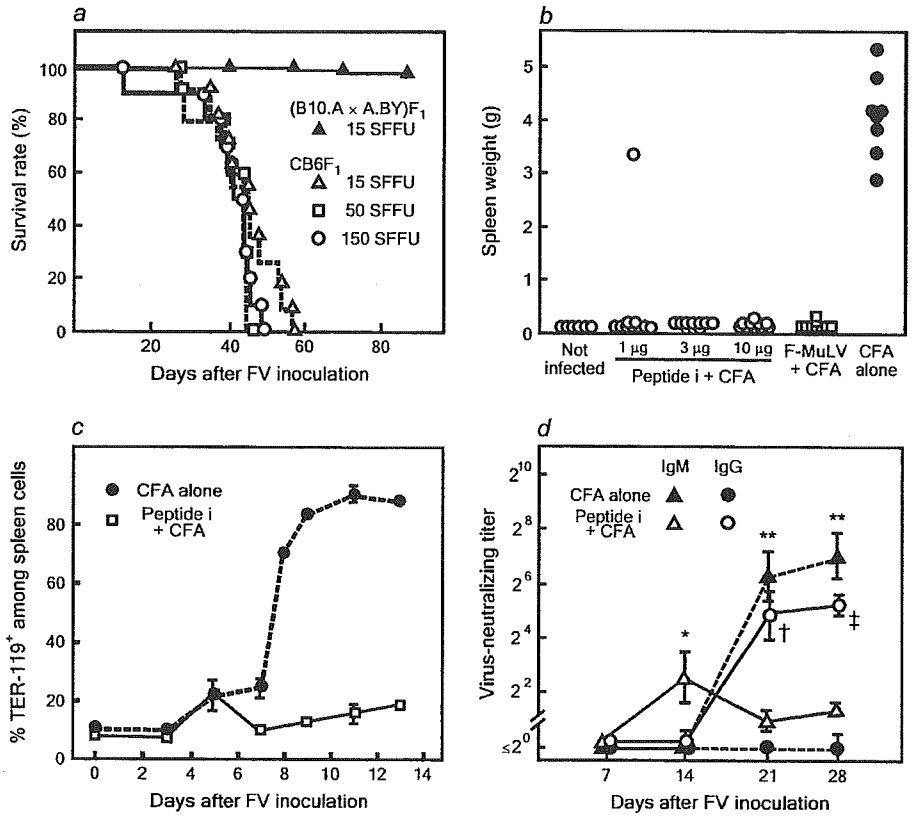

Fig. 1. Development of FV-induced disease in $CB6F_1$ mice and its prevention by immunization with the single-epitope peptide i. (a) $CB6F_1$ mice were inoculated intravenously with 15 ($n = 11$), 50 ($n = 10$) or 150 SFFU ($n = 10$) of FV and the survival of infected animals was examined. Similar curves were obtained in three repeated experiments. For a comparison, $(B10.A \times A.BY)F_1$ ($n = 40$) mice were also infected with 15 SFFU of FV and followed for their survival until PID 90. (b) The effect of different doses of peptide i on protective immunity against FV. $CB6F_1$ mice were immunized once with 1, 3 or 10 μg per mouse of peptide i in CFA, or given a CFA emulsion of purified F-MuLV particles at 40 μg per mouse. The F-MuLV particles used had been inactivated by UV irradiation as described (19). Control mice were given CFA without any peptide (CFA alone). Mice were challenged with 150 SFFU FV 4 weeks after immunization, and their spleen weight was measured as soon as they died (CFA alone group) or were killed at PID 45. Significant differences in spleen weights were only observed between the CFA alone group and five other groups ($P < 0.006$). (c) Changes in the percentages of TER-119⁺ erythroid cells among nucleated spleen cells of FV-infected $CB6F_1$ mice. Mice were immunized once with 10 μg (5 nmol) of peptide i in CFA or given CFA alone and inoculated with FV 4 weeks later. Each data point shows mean ± SEM calculated by using four to five individual mice per group. (d) Changes in serum titers of virus-neutralizing IgM and IgG antibodies after FV infection. $CB6F_1$ mice were either immunized once with 10 μg per mouse peptide i in CFA or given CFA alone, and challenged with 150 SFFU FV 4 weeks later. Each data point shows mean ± SEM calculated by using seven to eight individual mice per group. Serum titers of F-MuLV-neutralizing IgM and IgG were compared by paired *t*-test: *IgM titers are significantly higher than IgG titers at $P < 0.05$; **$P < 0.0001$. †, IgG titers are significantly higher than IgM titers at $P < 0.05$; ‡, $P < 0.01$.

$CB6F_1$ mice, $CD4^+$ and $CD8^+$ T cells were purified from $CB6F_1$ mice at 3 weeks after a single immunization with peptide i, and re-stimulated *in vitro* in the presence of syngeneic, γ-irradiated spleen cells as antigen-presenting cells (APCs). As shown in Fig. 2(a), $CD4^+$ T cells purified from the immunized $CB6F_1$ mice proliferated vigorously when stimulated with 1 μM of peptide i, while the proliferative responses of $CD4^+$ T cells purified from the control mice given CFA alone were below the background level even when stimulated with 20 μM of the same peptide. As controls, $CD8^+$ T cells purified either from the peptide-immunized or unimmunized control mice showed no significant proliferative responses even when stimulated with 20 μM peptide i.

To determine the minimal amount of the peptide that is required for the effective induction of protective immunity against FV infection, three different amounts of peptide i were given as a single intradermal immunization to $CB6F_1$ mice, and immunized mice were challenged with 150 SFFU FV. Since most of the unimmunized $CB6F_1$ mice died by PID 45 (Fig. 1a), infected mice were either dissected soon after their death or killed at PID 45, and their spleen weight was measured. As shown in Fig. 1(b), a single immunization with 3 μg (1.7 nmol) per mouse of peptide i was as effective as 10 μg per mouse of the same peptide, and only one mouse among the ten that were given 1 μg peptide i developed splenomegaly after FV infection. Thus, in the following experiments, 3–10 μg per mouse of peptide i was used as a sufficiently large protective dose.

FV-induced early splenomegaly is caused by the rapid growth and differentiation of SFFV-infected erythroid progenitor

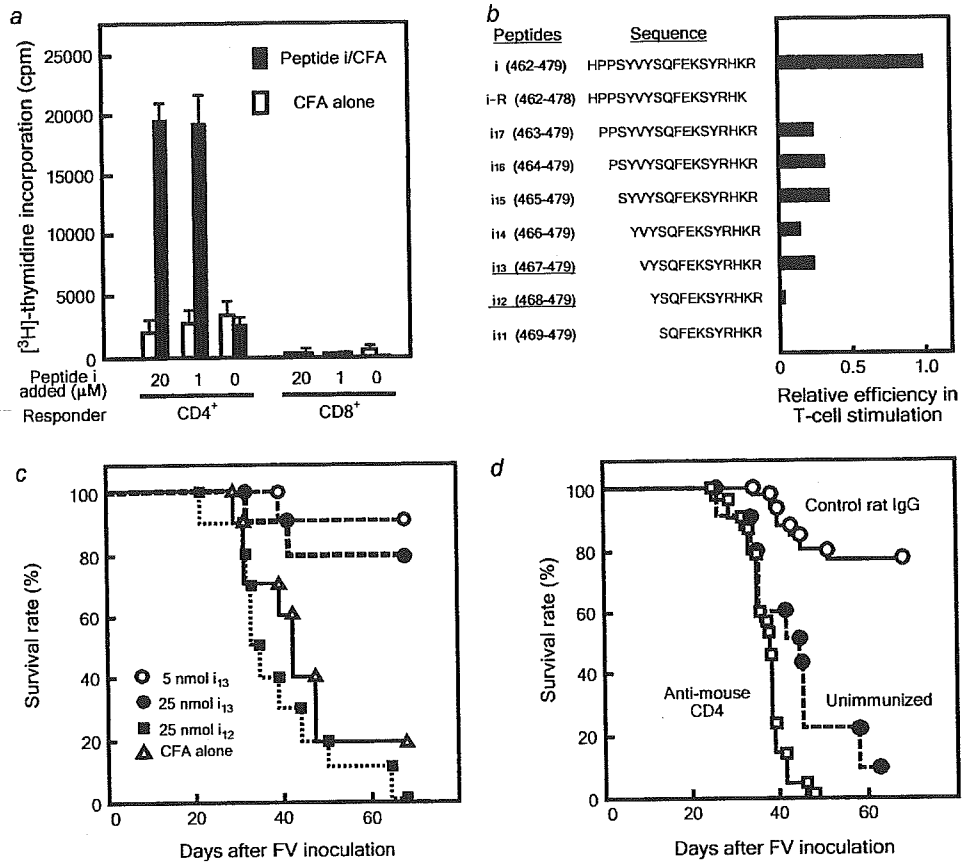

Fig. 2. Priming of CD4⁺ T cells by peptide immunization and efficacies in CD4⁺ T cell stimulation *in vitro* and immune protection *in vivo* of peptide i and its truncated derivatives. (a) Both CD4⁺ and CD8⁺ T cells were purified from the spleen of $CB6F_1$ mice at 3 weeks after a single immunization with 10 μg per mouse peptide i emulsified in CFA. Proliferative responses were measured 2 days after stimulation with the indicated concentration of peptide i along with syngeneic, γ-irradiated spleen cells as APCs. CD4⁺ and CD8⁺ T cells purified from $CB6F_1$ mice given CFA without a peptide (CFA alone) were used as controls. Data shown are averages + SEM of triplicate cultures, and the experiments were performed three times with essentially the same results. (b) Sequences of peptide i and its truncated derivatives, and their relative efficiency to stimulate FV-specific T cell clones. Representative data obtained with clone F5-5 are shown, while the data obtained with clone FP7-11 were consistent with those presented here. ED_{50} of the full-length i was 0.2 μM. (c) Protection of $CB6F_1$ mice against FV infection with the truncated peptide. $CB6F_1$ mice ($n = 10$ per group) were immunized once with 5 nmol per mouse of peptide i_{13}, 25 nmol per mouse of i_{13} or 25 nmol per mouse of i_{12}. Control mice were given CFA emulsion containing no peptide. Four weeks later, they were inoculated with 150 SFFU FV and followed for their survival. (d) $CB6F_1$ mice ($n = 22$ per group) were immunized once with 3 μg per mouse of peptide i and repeatedly injected with the anti-CD4 mAb (□) or control rat IgG (○). Four weeks after immunization, these mice and a group of unimmunized control mice (●) were inoculated with 150 SFFU FV and followed for their survival.

cells, and the resultant erythroblasts and maturing red cells are marked by mAb TER-119 (27). Thus, bursting of the TER-119⁺ erythroid cells was observed in the unimmunized control mice starting from PID 7, following the slow initial increase of the same cell population (Fig. 1c). On the other hand, the number of TER-119⁺ erythroid cells in the spleen started to decrease between PID 5 and 7 in the $CB6F_1$ mice that had been immunized once with peptide i. Virus-neutralizing antibodies in the serum were not detectable at PID 7 in FV-infected $CB6F_1$ mice regardless of whether they had been immunized with peptide i or not (Fig. 1d). In the $CB6F_1$ mice immunized with peptide i, virus-neutralizing IgM became detectable by PID 14, and the antibodies switched to IgG between PID 14 and 21. In the unimmunized mice, however, virus-neutralizing antibodies became detectable at PID 21, a week later than in the peptide-immunized mice, and they did not switch to IgG even at PID 28. These results indicated that the FV-induced expansion of erythroid cells was prevented in the peptide-immunized mice before virus-neutralizing antibodies became detectable in the serum.

Protection against FV disease correlates with CD4⁺ T cell stimulation

To identify the minimal effective sequence of the peptide vaccine, a series of truncated peptides were compared for their *in vitro* T cell-stimulating and *in vivo* protection efficacies (Fig. 2b and c). It was clear that the C-terminal Arg residue was indispensable for the recognition of this epitope by T cells. In fact, a 17-mer peptide, i-R, that lacked only the C-terminal

Arg totally lost the ability to stimulate $CD4^+$ T cell proliferation *in vitro*, while another 17-mer, i_{17}, that retained the Arg residue but lacked the N-terminal His kept the ability, albeit less efficiently than peptide i, to stimulate the T cells. When N-terminal residues were further removed from the 18-mer i and their efficacy to stimulate the $CD4^+$ T cells was examined through the range of concentrations between 0.01 and 20 μM, the 13-mer (i_{13}) retained the T cell-stimulating activity and showed a stimulatory effect comparable to peptide i_{17}, while the 12-mer (i_{12}) showed a stimulatory effect <1/24 of that of the full-length peptide i. Peptide i_{11} did not induce significant proliferation even when as much as 20 μM was added to the culture. In line with this result, the 13-mer retained the ability to induce protection against FV challenge in immunized $CB6F_1$ mice, while the 12-mer did not protect the same strain of mice against FV-induced disease even when five times more molecules were administered (Fig. 2c).

The requirement of $CD4^+$ T cells for the peptide-induced immune protection was further confirmed by depleting $CD4^+$ T cells from vaccinated $CB6F_1$ mice. The adopted schedule of the antibody administration resulted in undetectable $CD4^+$ T cells in the spleen in separately examined uninfected animals for a period equivalent to PID 0–14, and lack of $CD4^+$ T cells in the peripheral blood was confirmed in the vaccinated and infected group on PID 3–13 (data not shown). Antibody-induced depletion of $CD4^+$ T cells abrogated the efficacy of peptide immunization, and $CD4^+$ T cell-depleted animals died even more rapidly than the unimmunized control mice ($P < 0.05$). Injection of the control rat IgG did not affect the protective efficacy of the peptide vaccine, and ~80% of the peptide-immunized $CB6F_1$ mice that had been given the control antibody survived past PID 60 (Fig. 2d).

Peptide-induced immune protection against FV-induced disease in $CB6F_1$ mice genetically lacking a single component of the immune system

To examine possible effectiveness of the peptide immunization in mice genetically lacking either $CD8^+$ T or B cell components of the immune system, we produced $CB6F_1$ mice with a homozygous disruption of the $\beta_2 m$ gene or of the Ig μ-chain gene. The absence of $CD8^+$ T or B lymphocytes, respectively, was confirmed by flow cytometric analyses of the spleen and PBMCs (data not shown). In accordance with the prior experiments (Figs 1 and 2), ≥80% of the wild-type $CB6F_1$ mice were protected against FV infection when immunized with peptide i. Protective efficacy of the 13-mer peptide, i_{13}, was further confirmed, and the development of early splenomegaly was prevented in 70% of the $CB6F_1$ mice given i_{13} (Fig. 3a). Surprisingly, when $CB6F_1$-$\beta_2 m^{-/-}$ mice lacking $CD8^+$ T cells were immunized with peptide i, only <30% of the immunized mice developed splenomegaly and >70% survived until PID 100 in repeated experiments (Fig. 3). The observed survival curves were not significantly different between the peptide-immunized wild-type and $\beta_2 m^{-/-}$ groups ($P > 0.4$), indicating a similar effectiveness of the peptide vaccine both in the presence and absence of $CD8^+$ T cells. On the other hand, when the mice of the same susceptible $CB6F_1$ background that lacked B cells due to the homozygous *μMT* mutation were immunized with peptide i, they developed splenomegaly and all died by PID 100, indicating crucial roles of B cells for the peptide-induced immune protection. Interestingly, however, the temporal changes in the incidences of splenomegaly and leukemic death delayed significantly in repeated experiments in the peptide-immunized, B cell-deficient mice compared with those in the unimmunized control mice of the same deficiency (Fig. 3c and f). The delay in the development of splenomegaly in the peptide-immunized *μMT/μMT* mice was also substantiated by flow cytometric enumerations of FV-infected erythroid cells: at PID 7, 28.2 ± 3.7% ($n = 5$) of the nucleated spleen cells were positive for both TER-119 and F-MuLV gp70 in the unimmunized control mice, while the proportion of the TER-119⁺, gp70⁺ cells in the spleen was significantly smaller ($P < 0.05$) 12.1 ± 8.2% ($n = 5$) in the peptide-immunized *μMT/μMT* mice. The effect of peptide immunization was more striking in the bone marrow where the percentage of TER-119⁺, gp70⁺ cells in the unimmunized mice was 11.1 ± 4.4%, while that of the peptide-immunized mice was 0.72 ± 0.22% ($P < 0.03$) at PID 7. These results indicate some functions of non-B cells in delaying the FV-induced disease development.

Elimination of FV-producing cells from the spleen and bone marrow in the $\beta_2 m^{-/-}$ mice immunized with peptide i

We next compared the numbers of FV-infected cells between peptide-immunized and unimmunized control mice using infectious center assays. The relative ratio in the number of FV-producing cells in the spleen between the peptide-immunized and unimmunized mice started to decrease at PID 8 as observed in the previous experiments (13, 14), and FV infectious centers became undetectable by our assays by PID 28 in peptide-immunized wild-type mice (Fig. 4a). The lack of detectable FV-producing cells in the spleen of all the tested, peptide-immunized $CB6F_1$ mice was confirmed by seeding the cells prepared from the entire spleen ($>10^8$) of each animal as infectious centers at PID 28. The number of FV-producing cells in the bone marrow was also significantly lower in the peptide-immunized wild-type mice than in the unimmunized control mice at PID 8, 14 and 21, and became undetectable at PID 28 (Fig. 4d). At PID 28, 2.1×10^7 bone marrow cells were tested from each mouse and no infectious centers were detectable by our assays in any of the examined animals. In the $CB6F_1$-$\beta_2 m^{-/-}$ mice, the numbers of FV-producing cells in the spleen and bone marrow were significantly lower in the peptide-immunized than in unimmunized control mice at PID 14 and 28 (Fig. 4b and e), in accordance with the observed effectiveness of the peptide immunization in preventing the FV-induced disease development in the absence of $CD8^+$ T cells (Fig. 3). It should be noted that in seven of the nine immunized animals tested at PID 28 no infectious centers were detectable even when the cells of the entire spleen were inoculated into the culture. However, there were also individuals among the peptide-immunized $\beta_2 m^{-/-}$ mice in which FV-producing cells were still detectable in the spleen or bone marrow at PID 28 (Fig. 4b and e), while such cells were not detectable in any of the immunized wild-type mice tested at the same time point. These results imply that $CD8^+$ T cells were not necessarily required but may play some roles in the elimination of virus-infected cells in peptide-immunized $CB6F_1$ mice.

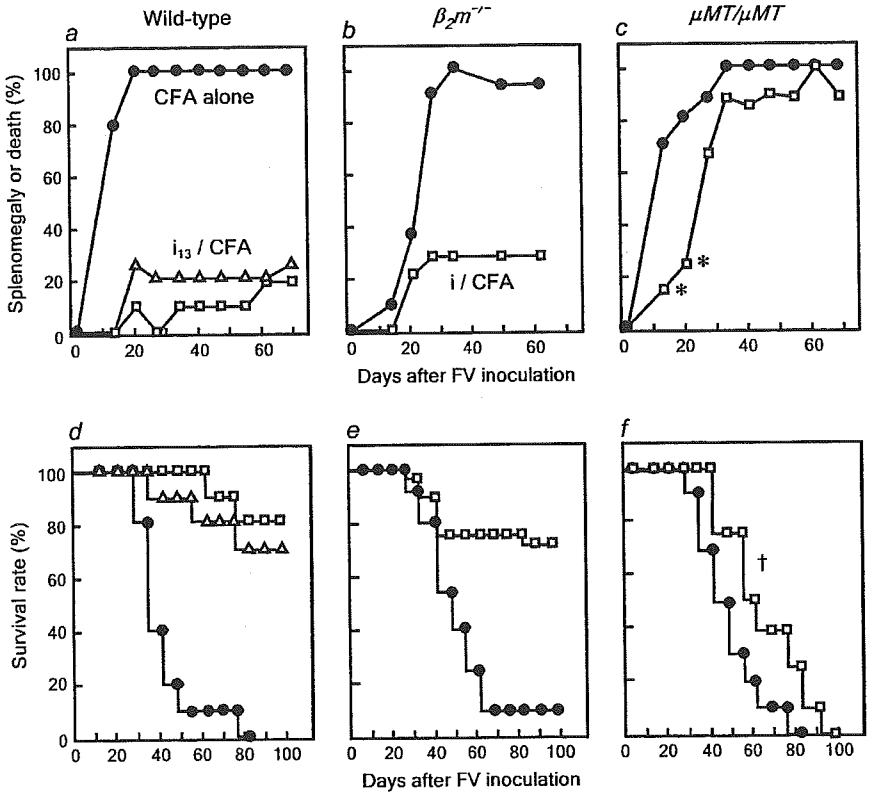

Fig. 3. Effects of immunization with peptide i on the development of FV-induced disease in $CB6F_1$ mice lacking $CD8^+$ T or B cells. Wild-type $CB6F_1$ mice (a and d), $CB6F_1$ mice lacking $CD8^+$ T cells due to homozygous targeting of the β_2m gene (b and e) and $CB6F_1$ mice lacking B cells due to homozygous targeting of the membrane exon of Ig μ-chain gene (c and f) were either immunized with 10 μg per mouse of peptide i in CFA (□) or given CFA alone (●). Another group of the wild-type mice were immunized with 10 μg per mouse of peptide i_{13} in CFA (Δ). Four weeks later, they were inoculated with 150 SFFV FV and followed for the development of splenomegaly and leukemic death. In (c), * indicates significant differences in the frequency of splenomegaly between the immunized and control groups ($P < 0.001$), and in (f), † indicates significant difference between the two survival curves ($P = 0.041$). The number of animals in each group were: (a) and (d), □, 10; Δ, 10; ●, 10; (b) and (e), □, 23; ●, 20 and (c) and (f), □, 12; ●, 16. The experiments were performed twice with essentially identical results.

In accordance with the lack of protection against FV-induced disease development, virus-producing cells constantly increased between PID 5 and 21 in the spleen and bone marrow of the $CB6F_1$-*μMT/μMT* mice, regardless of whether the hosts were immunized with peptide i or not. Interestingly, however, the numbers of virus-producing cells both in the spleen and bone marrow were significantly lower in the peptide-immunized, B cell-deficient mice than those in the unimmunized control mice of the same deficiency at PID 8 (Fig. 4f). This observation is consistent with the significant delay in the development of early splenomegaly and leukemic death (Fig. 3), and smaller numbers of $TER\text{-}119^+$ and viral $gp70^+$ FV-infected erythroid cells in the spleen and bone marrow in peptide-immunized, B cell-deficient $CB6F_1$ mice.

Priming and re-activation of $CD4^+$ T cells in the peptide-immunized μMT/μMT mice

To examine the possibility that the observed inefficiency in anti-FV protection of the immunization with peptide i in $CB6F_1$-*μMT/μMT* mice might be due to the lack of APC activity, rather than antibody-producing function, of B lymphocytes, peptide-specific proliferative responses were compared between the wild-type and *μMT/μMT* animals. When $CD4^+$ T cells purified from the wild-type $CB6F_1$ mice previously immunized with peptide i were used as responders, irradiated spleen cells both from the wild-type and from the *μMT/μMT* animals induced strong proliferative responses, although the peptide-specific proliferation was significantly weaker when *μMT/μMT* instead of the wild-type spleen cells were used as APC (Fig. 5a). FV infection significantly affected the APC function of wild-type spleen cells, but that of *μMT/μMT* spleen cells was not significantly reduced when used at PID 10. Similar results were observed when $CD4^+$ T cells purified from immunized *μMT/μMT* animals were used as responders. Thus, $CD4^+$ T cells were primed with peptide i in the absence of B cells, and spleen cells from *μMT/μMT* animals could present the peptide antigen to primed $CD4^+$ T cells, albeit less efficiently than the wild-type spleen cells, even after FV infection. Successful priming of $CD4^+$ T cells and their re-activation upon FV infection in *μMT/μMT* animals were further confirmed *in vivo* by analyzing the expression of an early activation marker, CD69, on T cells. Upon FV infection of peptide-immunized $CB6F_1$-*μMT/μMT*

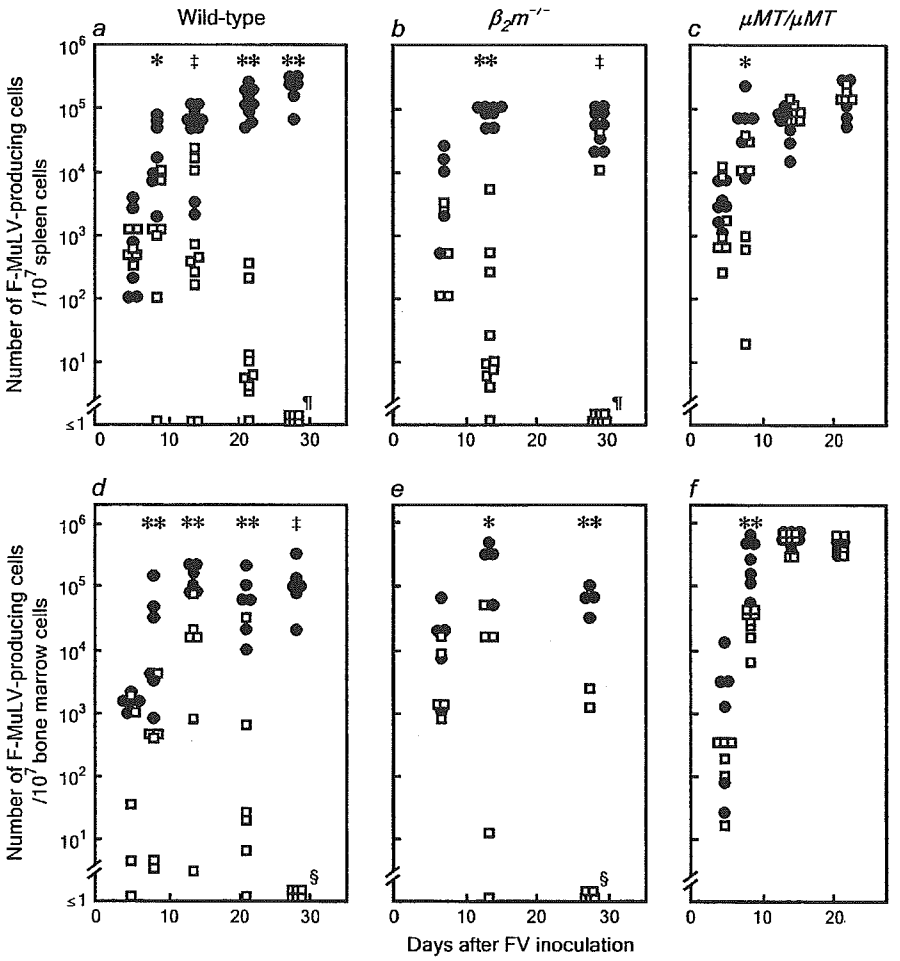

Fig. 4. Effects of immunization with peptide i on the number of FV-producing cells in $CB6F_1$ mice lacking $CD8^+$ T or B cells. Wild-type $CB6F_1$ mice (a and d), the $CB6F_1$ mice lacking $CD8^+$ T cells (b and e) and the $CB6F_1$ mice lacking B cells (c and f) were either immunized with 10 μg per mouse of peptide i in CFA (□) or given CFA alone (●). Four weeks later, they were inoculated with 150 SFFV FV and FV-producing infectious centers were enumerated in the spleen (a–c) and bone marrow (d–f). Each data point shows the actual number of infectious centers detected from each individual mouse. At least 10^7 spleen and bone marrow cells were tested from each animal. At PID 28, the cells prepared from the entire spleen ($>10^8$, ¶) and 2.1×10^7 (from wild-type mice) or 3.1×10^7 (from $\beta_2m^{-/-}$ mice) bone marrow cells (§) were inoculated as infectious centers to ensure the lack of detectable virus-producing cells. Infectious centers were undetectable from any of the tested animals indicated with ¶ or § at PID 28. Statistical significance of the difference between the immunized and unimmunized groups at each time point was examined: $*P < 0.04$; $**0.001 < P < 0.01$; ‡, $0.0002 < P < 0.001$.

mice, an increase in the proportion of $CD69^+$ cells among $CD4^+$ T cells was readily detectable (Fig. 5b). The percentages of $CD69^+$ cells among $CD4^+$ T cells in the spleen at PID 7 were significantly higher in the peptide-immunized than in the unimmunized animals, indicating re-activation of peptide-primed T cells upon FV infection (Fig. 5c). The effect of peptide immunization on the induction of CD69 expression was even more pronounced when bone marrow cells were tested (Fig. 5d). Interestingly, the $CD69^+$ population among $CD8^+$ T cells also showed a significant increase when peptide-immunized and unimmunized *μMT/μMT* mice were compared at PID 7, confirming the previously demonstrated activation of $CD8^+$ cytotoxic cells at PID 7 (14).

Production and class switching of serum antibodies reactive to the surface of FV-induced leukemia cells in the peptide-immunized mice

Although virus-neutralizing antibodies were not detectable in FV-infected animals until PID 14 (Fig. 1d), non-neutralizing anti-FV antibodies might have been produced at earlier time points, and might have contributed to the observed decrease in the number of FV-infected cells in the vaccinated animals, which was evident at as early as PID 7 (Figs 1c and 4). Thus, the possible presence of anti-FV antibody in the serum was examined using FV-induced leukemia cells as indicators. The hemisyngeneic ($H2^{b/b}$), FV-induced leukemia cells Y57-2C expressed both the F-MuLV *gag* and *env* gene products as

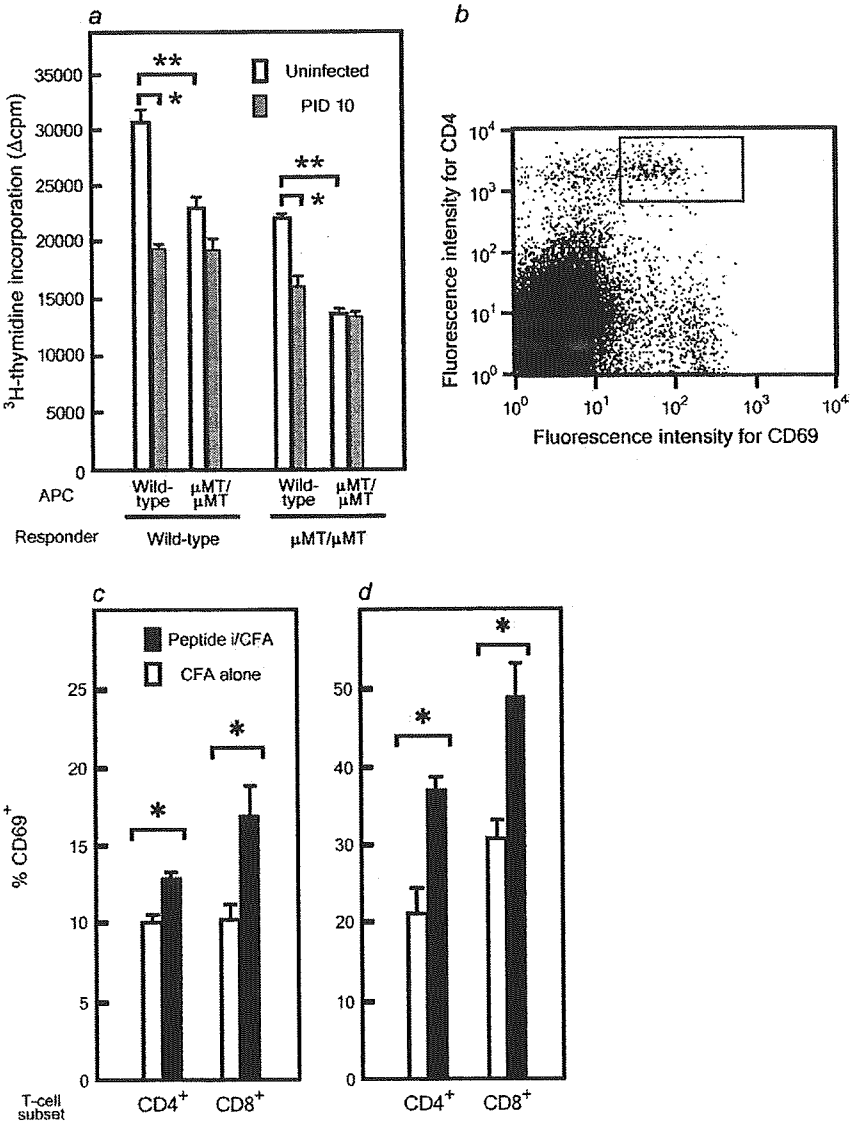

Fig. 5. Priming and re-activation of CD4$^+$ T cells with peptide i in the B cell-deficient mice. (a) CD4$^+$ T cells were purified from the spleen of wild-type and homozygous *μMT/μMT* CB6F$_1$ mice at 3 weeks after a single immunization with 10 μg per mouse peptide i emulsified in CFA. Proliferative responses were measured at 2 days after stimulation with 1 μM peptide i along with the indicated APC. Spleen cells as APC were prepared from the wild-type and *μMT/μMT* CB6F$_1$ mice either without FV inoculation or at PID 10, and γ-irradiated. The magnitude of antigen-specific proliferation is shown by Δ counts per minute (c.p.m.) in this chart by subtracting the average [^{3}H]thymidine ([^{3}H]TdR) incorporation into the cultures containing no peptide from that in the peptide-containing cultures. Levels of [^{3}H]TdR incorporation into the cultures without a peptide were <120 c.p.m. Data shown are averages + SEM of triplicate cultures, and the experiments were performed twice with essentially the same results. *, significantly different at $P < 0.01$; **$P < 0.001$. (b) A representative pattern of CD69 expression on CD4$^+$ T cells in the bone marrow of the *μMT/μMT* mice previously immunized with peptide i. The small rectangle indicates the gate used to calculate the percentage of CD69$^+$ cells among CD4$^+$ T cells. (c) and (d) Comparison of the percentages of CD69$^+$ activated cells among CD4$^+$ and CD8$^+$ T cells in the spleen (c) and bone marrow (d) at 7 days after FV inoculation between the peptide-immunized and unimmunized *μMT/μMT* mice. Data are averages + SEM calculated with five mice per group. *, the percentage of CD69$^+$ population is significantly higher in the immunized than in the unimmunized mice at $P < 0.005$.

well as SFFV gp55 on their surfaces (Fig. 6a). Sera from FV-infected CB6F$_1$ mice bound onto the surface of Y57-2C cells, and geometric means of the fluorescence intensities decreased in proportion to serum dilutions (Fig. 6b). Therefore, at each time point titers of serum antibodies reactive to the surface of the FV-induced leukemia cells, designated hereinafter anti-leukemia cell antibody titers, were determined by dividing geometric means of fluorescence intensities obtained by incubating the indicator cells with a 1/16 dilution of serum samples by the geometric mean of fluorescence intensities obtained with the same dilution of pooled control serum collected from uninfected CB6F$_1$ mice. Interestingly,